

# EFFECT OF INTERFACIAL THERMAL MISMATCH ON INTERFACIAL STRENGTH OF COMPOSITES<sup>①</sup>

Liu Ruoyu

*Beijing Institute of Aeronautical Materials, Beijing 100095*

Wang Lingsen, Zhang Jinsheng, Fan Yi

*The Research Institute of Powder Metallurgy,*

*Central South University of Technology, Changsha 410083*

**ABSTRACT** By means of diamond microdebonding test method and the interfacial stress field finite element analysis (FE), the influence of interfacial thermal expansion mismatch between fiber and matrix on the interfacial strength was investigated. The results show that, the radial thermal mismatch has played a dominant role, with the influence of the axial thermal mismatch being relatively small. Furthermore, the interfacial thermal residual stress was also studied.

**Key words** composite interfacial thermal mismatch interfacial strength

## 1 INTRODUCTION

Due to the difference of the thermal expansion mismatch between the fibers and the matrix, there always exists thermal residual stress remaining in composites as a result of the nonuniformity of the thermal deformation when the composites cool from high temperature to room temperature.

Furthermore, this kind of thermal residual stress, coupling with the external load, makes the interfacial stress field more complicated. This paper, focusing on interfacial thermal mismatch, will investigate its effect on the interfacial strength of composites in details. Here, the interfacial thermal mismatch is defined as the difference in thermal expansion coefficients (CTE) between the fiber and the matrix, including the radial mismatch,  $\Delta\alpha_r (= \alpha_m - \alpha_{fr})$ , and the axial mismatch,  $\Delta\alpha_a (= \alpha_m - \alpha_{fa})$ , where  $\alpha_m$  is the thermal expansion coefficient of the matrix, and  $\alpha_{fr}$  and  $\alpha_{fa}$  are the fiber's radial and axial CTEs respectively. The effect of both mismatches on the interfacial strength will be discussed in the following paper.

## 2 EXPERIMENTAL

To investigate a variety of composites with different interfacial mismatches, nine kinds of unidirectional fiber reinforced glass-ceramic composite pre-pregs were made by conventional slurry-impregnation method, adopting the Nicalon SiC fiber, T300-3K carbon fiber and carbon filament as reinforcements, and using 7740 (Corning code) borosilicate glass and self-made LAS I, LAS II, LAS III lithium aluminosilicate glass-ceramic powders as matrices. The properties of the fibers and the compositions of the matrices are shown in Table 1 and Table 2. The pre-pregs were then dried, and hot pressed at 1200 °C in graphite die under nitrogen gas protection.

By using samples of size 5 mm × 5 mm × 15 mm of each non-reinforced matrix produced under the same conditions as the corresponding composite, the average thermal expansion coefficients (CTEs) of the matrices were determined in air on a DL-1500 thermal dilatometer with the temperature ranging from 50 °C to 1000 °C at a heating and cooling rate of 10 °C/min. The resultant thermal expansion coefficients of matrices

① Supported by the National Natural Science Foundation of China

Received Jul. 1, 1996; accepted Nov. 12, 1996

**Table 1 Properties of fibers**

Fiber	Diameter / cm	Density / $\text{g} \cdot \text{cm}^{-3}$	Tensile strength / MPa	Young's modulus / GPa	Tangential poisson ratio/ $\nu_{r\theta}$	Thermal expansion coefficient / $10^{-6} \text{ } ^\circ\text{C}^{-1}$
Nicalon SiC	10~ 15	2.55	240	200	0.2	3.1
T300-3 K	5~ 7	1.74	333	235	0.2	- 0.7(radial) , 0.3(axial)
C filament	5~ 6	1.76	240	250	0.25	10.1(radial) , 0.1(axial)

**Table 2 Fundamental chemical compositions and properties of matrices**

Matrix	Chemical composition/ %									Young's modulus / GPa	Poisson ratio
	Li <sub>2</sub> O	Al <sub>2</sub> O <sub>3</sub>	SiO <sub>2</sub>	B <sub>2</sub> O <sub>3</sub>	Na <sub>2</sub> O	K <sub>2</sub> O	P <sub>2</sub> O <sub>5</sub>	TiO <sub>2</sub>	CaO		
7740			80.2	12.5	4.0		2.0	0.6		63	0.2
LAS I	8.9	30.4	53.7			1.0	4.0	2.0		77.7	0.3
LAS II	7.5	25.5	60.0			1.0	4.0	2.0		81.2	0.3
LAS III	4.5	15.5	73.0			1.0	4.0	2.0		70.7	0.3

were included in Table 3.

The determination of interfacial debonding forces were conducted on the self-made microdebonding device. By means of finite element analysis, the transient stress distribution along the interface was calculated. For conducting finite element analysis, it is necessary to make the following assumptions:

**Table 3 Resultant thermal expansion coefficients of matrices**

Matrices	7740	LAS I	LAS II	LAS III
CTEs/ $10^{-6} \text{ } ^\circ\text{C}^{-1}$	3.2	- 1.0	- 0.1	- 1.7

(1) Both the fiber and matrix are elastic in all directions;

(2) The bonding of fiber and matrix is perfect;

(3) There exists only frictional bonding at the interface;

(4) The thickness of the interfacial layer can be neglected;

(5) The applied load is totally acted on the fiber end axially;

(6) The axes of the cylindrical fibers are vertical to the sample surface;

(7) A fixed boundary condition is applied to the analyzed matrix and equivalent composite.

To meet the above conditions, samples were made as thin as possible, and the pyramidal indenter tip was accurately acted on the center of

the fiber end.

### 3 RESULTS AND ANALYSES

There are two methods for calculation of interfacial strength, one of which takes the interfacial stress as constant, the interfacial strength being characterized as the mean value of shear stress along the fiber axis, while the other takes assumptions that the stresses along the interface are not uniformly distributed and the interface fails at the maximum interfacial stress, the interfacial strength being figured out according to the interfacial maximum shear stress criteria or the maximum radial tensile stress criteria<sup>[2]</sup>. In this study the later is adopted.

According to the calculation results of interfacial shear strength,  $\tau$ , and the calculated interfacial thermal mismatches shown in Table 4, the relationship between interfacial strength and radial thermal mismatch is obtained, as illustrated in Fig. 1, with a few data in ref. [2] included.

The experimental data, after undergoing computer regression analyses, can be plotted as Fig. 2 and expressed as

$$\lg \tau = 0.0655 \Delta \alpha_r + 1.9444 \quad (1)$$

From Fig. 1, it can be seen that, there is an monotonic exponential relationship between the interfacial strength and the radial thermal mismatch  $\Delta \alpha_r$ .

Besides, to illustrate the influence of axial

Table 4    Interfacial thermal mismatches between fiber and matrix

Composite	Thermal expansion coefficient/ $10^{-6} \text{ }^{\circ}\text{C}^{-1}$			Thermal mismatch/ $10^{-6} \text{ }^{\circ}\text{C}^{-1}$	
	$\alpha_{\text{fr}}$	$\alpha_{\text{fa}}$	$\alpha_{\text{m}}$	$\Delta\alpha_{\text{r}}$	$\Delta\alpha_{\text{a}}$
C/LAS I	10.1	0.1	− 1.0	− 11.1	− 1.1
C/LAS II	10.1	0.1	− 0.1	− 10.2	− 0.2
C/7740	10.1	0.1	3.2	− 6.9	3.1
SiC/LAS III	3.1	3.1	− 1.7	− 4.8	− 4.8
SiC/LAS I	3.1	3.1	− 1.0	− 4.1	− 4.1
SiC/LAS II	3.1	3.1	− 0.1	− 3.2	− 3.2
T300/LAS III	− 0.7	0.3	− 1.7	− 1.0	− 2.0
SiC/7740	3.1	3.1	3.2	0.1	0.1
T300/7740	− 0.7	0.3	3.2	3.9	2.9

thermal mismatch,  $\Delta\alpha_{\text{a}}$ , on the interfacial strength,  $\tau$ , a dotted figure is plotted as Fig. 3. It can be found that, there doesn't exist a distinct relationship between the interfacial strength,  $\tau$ , and the axial thermal mismatch,  $\Delta\alpha_{\text{a}}$ , which implies that the interfacial strength,  $\tau$ , is mainly affected by the radial thermal mismatch,  $\Delta\alpha_{\text{r}}$ .

4    DISCUSSION

4. 1    Relations between  $\Delta\alpha_{\text{r}}$  and interfacial strength

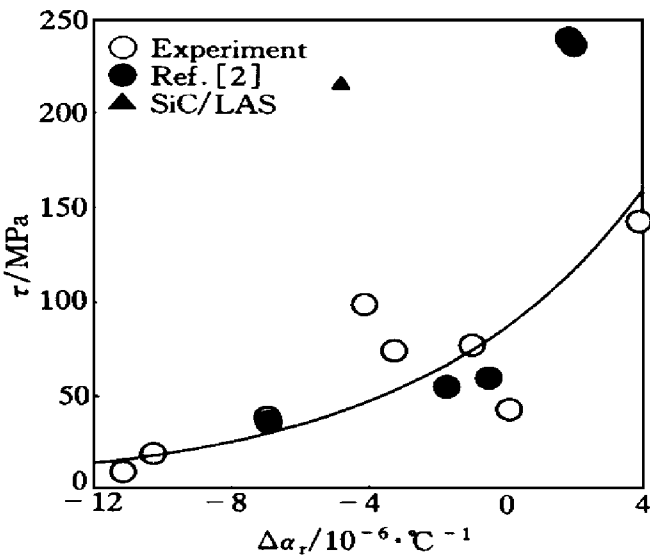


Fig. 1    Relationship of interfacial strength versus radial thermal mismatch ( $\Delta\alpha_{\text{r}}$ )  
“○” denotes experimental data, and “ref. [2]” and “SiC/LAS” represent data from ref. [2] and uncommon data point of SiC/LAS III

The phenomenon that the interfacial strength,  $\tau$ , increases with increasing radial thermal mismatch  $\Delta\alpha_{\text{r}}$  may be explained as follows.

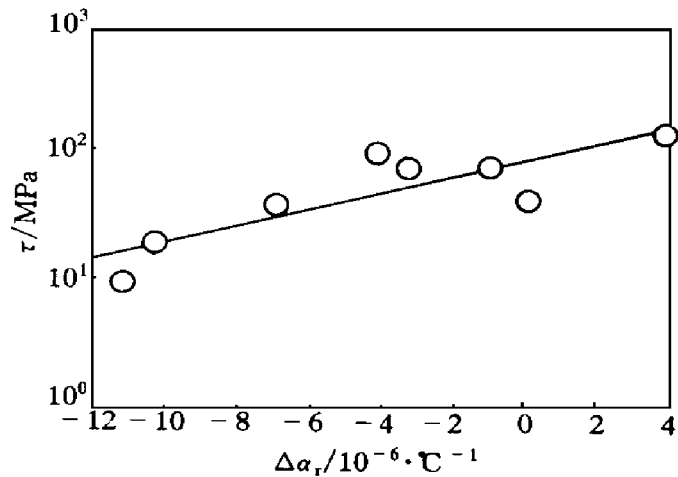
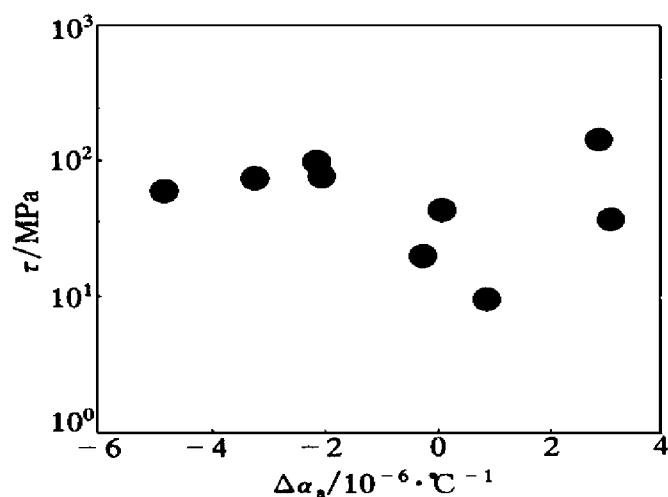


Fig. 2    Regression curve of interfacial strength,  $\tau$ , versus radial thermal mismatch,  $\Delta\alpha_{\text{r}}$

When the composite is cooled down from its hot pressing temperature, if  $\Delta\alpha_{\text{r}}$  and  $\alpha_{\text{m}}$  are both negative but  $\alpha_{\text{fr}}$  is positive, the matrix will expand and the fiber will contract radially and then at the interface there will occur a separating tendency as the result of radial tensile stress originated from the fiber and the matrix respectively. If the interfacial bonding is not sufficiently strong and just consists mainly of mechanical clamping stress, then the thermal deformation will pronouncedly weaken the mechanical clamping forces and thus bring about a relatively small interfacial strength.



**Fig. 3 Relationship between interfacial strength,  $\tau$ , and axial thermal mismatch,  $\Delta\alpha_a$**

For example, when C/LAS I and C/LAS II composites whose  $\Delta\alpha_r$  values equal  $-11.1 \times 10^{-6}$  and  $-10.2 \times 10^{-6} \text{ } ^\circ\text{C}^{-1}$ , respectively, are cooled from hot pressing temperature, the distances between the fiber and matrix due to thermal mismatch will be 30.8 and 26.5 nm respectively, calculated according to the equation<sup>[3]</sup> as below:

$$d(fc) = \Delta\alpha_r \cdot \Delta T \cdot R_f \quad (3)$$

where  $d(fc)$  means the relative distance of the fiber away from the matrix;  $\Delta T$  means the difference between the room temperature and the lowest temperature at which the matrix get relaxed;  $R_f$  represents the radius of fiber.

When  $\Delta\alpha_r$ ,  $\alpha_{fr}$  and  $\alpha_m$  are all negative, as  $\alpha_m > \alpha_{fr}$ , the matrix will expand more than the fiber, there will still exist a separating tendency along the interface. As an example, the T300/LAS III composite, calculated according to eq. (3),  $d(fc)$  is about 3 nm. If the interfacial bonding is relatively strong, then a tensile stress will show up at the interface; while if the interface is weak, the interfacial tensile stress will be relatively small, and the mechanical clamping force will be markedly decreased. So, only if  $\Delta\alpha_r < 0$ , there exists a separating tendency at the fiber/matrix interface with the result of a weakened interface and a relatively low interfacial strength when the composite cooled down from high temperature to room temperature. While if  $\Delta\alpha_r > 0$ , i. e.,  $\alpha_m > \alpha_{fr} > 0$ , both the

fiber and matrix will contract during cooling, with the contraction of matrix larger than that of fiber, resulting that the matrix will try to “embrace” the fiber, leading to a higher interfacial strength. With further increasing of  $\Delta\alpha_r$ , the interface will be compressed increasingly, with an enhancement of fiber debonding force and thus a large value of interfacial strength.

## 4.2 Distribution of interfacial stress field

Fig. 4 shows the distribution of interfacial radial stress,  $\sigma_{yy}$ , along the fiber axis direction when the fiber gets debonded from matrix in the composites with different values of  $\Delta\alpha_r$ , which further signifies that, when  $\Delta\alpha_r < 0$ , such as C/7740, C/LAS I, SiC/LAS II and SiC/LAS III there produces a larger radial tensile stress at the interface; while if  $\Delta\alpha_r > 0$ , as T300/7740, the stress acting on the fiber at the interface is a radial compressive stress, which enhances the ir

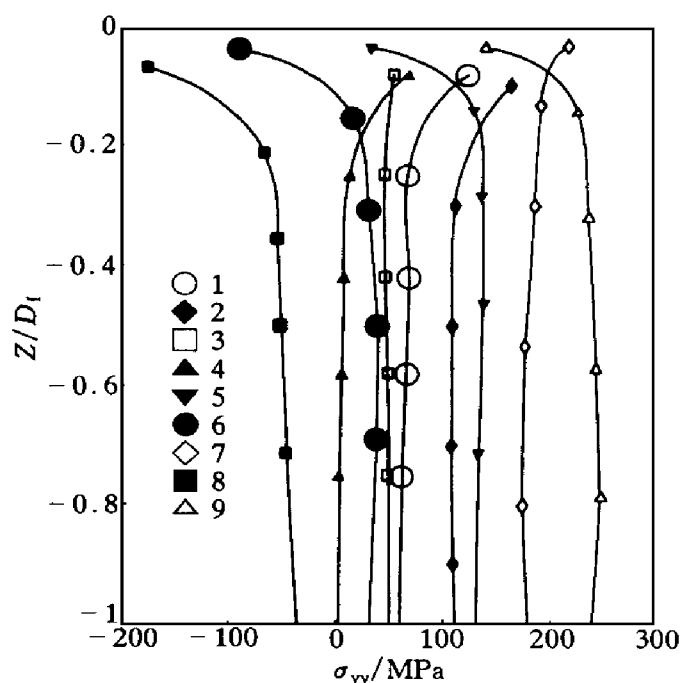


**Fig. 4 Distribution of transient interfacial radial stress  $\sigma_{yy}$  along fiber axis when debonding takes place, where  $Z/D_f$  represents ratio of depth from fiber free surface along interface to diameter of fiber ( $D_f$ )**

(Curves 1 to curve 9 denote C/7740, C/LAS I, C/LAS II, SiC/LAS I, SiC/LAS II, SiC/LAS III, SiC/7740, T300/7740, and T300/LAS III composites respectively.)

terfacial strength.

#### 4.3 Effect of interfacial radial thermal residual stress on interfacial strength

By utilizing a cylindrical model, the nominal thermal residual stress at the interface away from the free surface can be expressed as<sup>[2]</sup>

$$\sigma_{\text{res}} = \Delta\alpha_r \cdot \Delta T \cdot E_m / [1 + \nu_m + (1 - \nu_\theta) E_m / E_r] \quad (4)$$

where  $\sigma_{\text{res}}$  represents the thermal residual stress;  $E_r$  and  $\nu_m$  are Young's modulus and Poisson ratio of matrix, respectively;  $E_r$  and  $\nu_\theta$  are the radial Young's modulus and tangential Poisson ratio of fiber.

Fig. 5 shows the relationship between interfacial radial thermal residual stress via the inter-

facial strength,  $\tau$ . It can be seen that, with the interfacial radial thermal residual stress changing from negative to positive, i. e., from compressive stress to tensile stress, the interfacial strength tends to drop down, which is in agreement with the analysis results by radial thermal mismatch.

## 5 CONCLUSIONS

(1) Interfacial strength increases with the interfacial thermal mismatch increasing and there exists the following expression:

$$\lg \tau = 0.0655 \Delta\alpha_r + 1.9444$$

(2) The axial thermal mismatch doesn't have a pronounced effect on the interfacial strength.

(3) The interfacial strength is prominently affected by the interfacial radial thermal residual stress at the interface if the interfacial reactions can be neglected.

## REFERENCES

- 1 Aveston J, Cooper G A, Kelly A. In: Conf Proc, National Physical Laboratory, 1971: 15– 26.
- 2 Grande D H *et al.* J Mater Sci, 1989, 23: 311.
- 3 Phillips D C. J Mater Sci, 1974, 9: 1847.
- 4 Langley N R, LeGrow G E, Lipowitz J. In: Mazdiyasn K S ed, Fiber Reinforced Ceramic Composites —Materials, Processing and Technology, New Jersey: Noyes Publications, Park Ridge, 1990: 86.

(Edited by Peng Chaoqun)

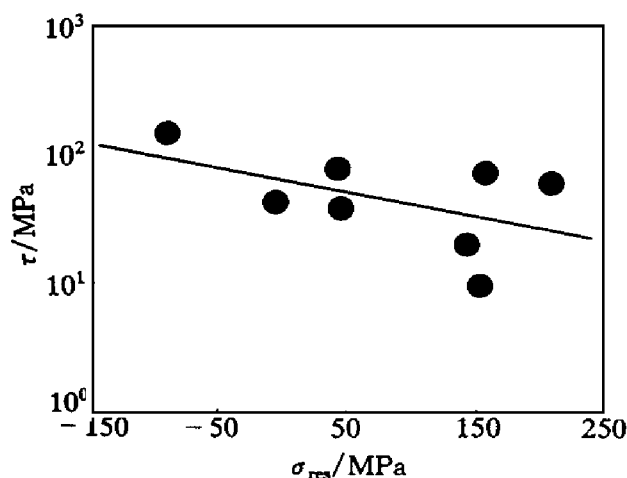


Fig. 5 Relationship between interfacial strength and interfacial radial stress